Novel Copper Loaded Core-shell Silica Nanoparticles With Improved Copper Bioavailability Synthesis, Characterization And Study Of Antibacterial Properties

2011

Pavithra Maniprasad
University of Central Florida

NOVEL COPPER LOADED CORE-SHELL SILICA NANOPARTICLES WITH IMPROVED COPPER BIOAVAILABILITY: SYNTHESIS, CHARACTERIZATION AND STUDY OF ANTIBACTERIAL PROPERTIES

by

PAVITHRA MANIPRASAD
B.Tech. Anna University, 2009

A thesis submitted in partial fulfillment of the requirements
for the degree of Master of Science
in the Burnett school of Biomedical Science
in the College of Science
at University of Central Florida
Orlando, Florida

Fall Term
2011

Major Professor: Swadeshmukul Santra

ABSTRACT

A novel core-shell silica based antimicrobial nanoparticle was synthesized. The Stöber silica shell has been engineered to accommodate copper. Synthesis of the core-shell Cu-silica nanoparticle (C-S CuSiNP) involves preparation of base-hydrolyzed Stöber silica "seed" particles first, followed by the acid-catalyzed seeded growth of the Cu-silica shell layer around the core. Scanning electron microscopy and transmission electron microscopy showed monodispersed, spherical shaped nanoparticles with smooth surface morphology. Characterization of particle size distribution in solution by the Dynamic Light Scattering (DLS) technique was fairly consistent with the electron microscopy results. Loading of Cu to nanoparticles was confirmed by the SEM-Energy Dispersive X-Ray Spectroscopy (EDS) and Atomic Absorption Spectroscopy (AAS). Antibacterial efficacy of C-S CuSiNP was evaluated against *E.coli* and *B.subtilis* using Cu hydroxide ("Insoluble" Cu compound) and copper sulfate as positive control and silica "seed" particles (without Cu loading) as negative control. Minimum Inhibitory Concentration (MIC) of C-S CuSiNP was evaluated by measuring the fluorescent intensity of resorufin to determine the decrease in viable cells with increase in copper concentration in C-S CuSiNP. The MIC value of C-S CuSiNP against both *E.coli* and *B.subtilis* was estimated to be 4.9 ppm. Bac-light fluorescence microscopy based assay was used to count relative population of the live and dead bacteria cells. Antibacterial study clearly shows that C-S CuSiNP is more effective than insoluble Cu hydroxide particles and copper sulfate at equivalent metallic Cu concentration, suggesting more soluble Cu in C-S CuSiNP material due to its core-shell design.

Keywords: core-shell nanoparticle, copper loaded silica, antibacterial, sol-gel, copper biocide.

I dedicate this work to my lovable family, especially my parents (Mrs. and Mr. Maniprasad) and my brother (Girish Kumar Maniprasad).

ACKNOWLEDGMENTS

I take this opportunity to express my heartfelt thanks to my professor, Dr.Swadeshmukul Santra, PhD for his consistent guidance enabling me to grasp the subject.

I would also like to acknowledge my committee members Dr.Saleh Naser and Dr.William Self for their valuable thoughts and suggestions which acted as a driving force for improving my work.

I thank my colleagues Roseline Menezes, Andrew Teblum and Jennelle Suarez for their generous help with which I was able to attain better results on the bacterial study and confocal microscope. I extend my thanks to my lab mates Astha Malhotra, Srijita Basumallick, Dr.Padmavathy Tallury for helping me in the course of the project. I appreciate the UCF-Materials Characterization Facility (MCF) Staff members for helping me with the material characterization.

I would like to thank my friends Sai, Jeshwanth, Prabhu, Mukundhan, Bihag, Priyadarshini, Priya, Ramya, Vidusha, Aarthi, Maha, Jagadeesh, Sai sathya, Vanathy, Rucha, Swetha, Bindu, Mona, Shanmugapriya, Bala for their encouragement, support and affection. I thank my family for their everlasting love and faith in me. Above all I would like to thank the Almighty for showering his blessings.

TABLE OF CONTENTS

LIST OF FIGURES

LIST OF TABLES

CHAPTER 1 INTRODUCTION

1.1 History of Copper

The biocidal properties of metal ions have been known for centuries. Copper is one of the widely known metals for its antimicrobial property since ancient times[1]. Copper was used to treat leg ulcers by Hippocrates, the father of medicine. Copper oxides and copper carbonates were used for treating skin diseases. Recent laboratory studies of *E.coli* inhibition by metals surfaces have shown copper to be the most effective. Copper is one of the groups of metallic elements which are essential to human health. It is estimated that the humans drink and eat about 1 milligram of copper per day[1]. Copper is widely being used in many medical (intrauterine) devices and hence considered safe to humans. Today copper is widely used as an antimicrobial agent in wood preservative[2], food packaging[3,4], as antifouling agents in paint based materials[5], water purifier[1], in healthcare facilities to provide microorganism-free surfaces[6,7] and in agriculture[8]. The mechanism by which copper is toxic to microorganisms is found to be through free radical generation, permeabilization of cell membrane, DNA and RNA degradation[1]. A recent report by Weaver et al. suggests that rapid killing of MRSA, Methicillin-Resistant Staphylococcus Aureus (antibiotic resistant bacterial infection) by exposure to Cu surface is due to compromised cellular respiration and DNA damage[9].

Copper compounds are widely used as bactericide / fungicide in agriculture to prevent plant diseases[10]. Commercially available biocides are oxides, hydroxides or chelates of copper. To obtain acceptable protection against infection, at least 8 to 10 applications per season is necessary[11]. Repeated applications of these formulations will result in copper accumulation in the soil posing threat to the environment[5,12-14].

1.2 Silica

Silicon is a naturally occurring mineral which can be seen in everyday life as beads packed to absorb moisture and control humidity. Silica gel has a wide use in chromatography techniques in chemistry. The use of silica in biomedical and biotechnological applications has been significant in the past few years. The MSDS of silica gel states it to be a non-toxic, non-flammable and stable material. However, if consumed it can cause acute or chronic illness. Silica can be synthesized into nanoparticles, transparent films and solid materials[15].

1.3 Silica Nanoparticles

Silica nanoparticles have become to be known as attractive host matrix due to its ease of surface modification, stability and inertness[16]. Silica based nanoparticles are used in bioanalytical applications where they are conjugated with bioanalytes for analyte detection and signaling[15]. Dye loaded silica nanoparticles are widely used in various biomedical applications[17]. Recently, Cornell University developed silica based fluorescent nanoparticles called “Cornell”

dots to detect cancer cells which have been approved by the FDA for phase 1 clinical trials in human subject [http://www.news.cornell.edu/stories/Jan11/CUdotsClinical.html].

Silica nanoparticles are synthesized mainly by micro emulsion method[18,19] or stö ber method[16,20-23]. Stö ber method is a one-step sol-gel method of synthesizing silica nanoparticles. It involves the condensation of tetraethylorthosilicate (TEOS) in ethanol and water mixture. Ammonia acts as a base catalyst to this reaction.[16]. It does not use any hazardous chemicals. Excellent control of particle size and shape can be achieved. Condensation reaction is followed by hydrolysis of ethoxy group in TEOS.

1.4 Copper Nanoparticles

Copper or copper oxide nanoparticles have been used for a wide range of antimicrobial applications. Copper nanoparticles are synthesized by inert gas condensation technique[24], electrolysis method[25], deposition of copper salts on to the matrix[26], copper salt reduction[27]. This enables in the production of nano size particles. But this can easily cause aggregation of the particles and deterioration of its chemical properties over a period of time resulting in reduced efficiency of its antimicrobial activity[26].

1.5 Copper-loaded Silica Nanoparticles

It is evident that usage of antimicrobial copper will continue to increase in the near future. The only way to reduce free copper accumulation and bring about its slow release over a period of time is to load copper on to a matrix. This will also help in maintaining its properties. In the present study our main goal is to reduce the amount of copper in the material without compromising antibacterial activities. This study is focused on efficient design of copper embedded silica nanoparticle delivery platform. It reports the different approaches to synthesize copper loaded silica nanoparticles, characterization of each material and their antibacterial property. As a novel approach, copper-loaded silica nanoparticles were synthesized based on core-shell design. The Core-shell copper loaded silica nanoparticles (C-SCuSiNP) are composed of pure silica core and copper loaded silica shell. Since copper is distributed in the NP shell region, reduced amount of copper will be required to obtain significant antibacterial efficacy. Furthermore, bioavailability of copper is expected to increase in C-SCuSiNP in comparison to any "insoluble" copper compound due to availability of more "soluble" Cu. Improving efficacy of Cu biocide has clear advantage of reducing undesirable burden related to Cu toxicity in the environment.

CHAPTER 2 MATERIALS AND METHODS

2.1 Materials

All reagents were purchased from commercial vendors and used without any further purification. Ethanol (95% V/V; Fisher Scientific), tetraethylorthosilicate (TEOS; Fisher Scientific), N-(Trimethoxy Silyl Propyl) - Ethylenediamine, Triacetic acid, Trisodium salt 45% in water (TSPETE; Fisher Scientific), ammonium hydroxide (NH_3 content 28 – 30 wt%; Sigma-Aldrich), concentrated hydrochloric acid (Fisher Scientific), copper sulfate pentahydrate (CQ concepts, Ringwood, IL), sodium chloride (Fisher Scientific). Kocide®3000, a product of DuPont ™ was received as a gift from Dr. Jim Graham (Citrus Research and Education Center, Lake Alfred, FL). Mueller-Hinton (MH) agar, Luria Bertani (LB) broth and agar for antibacterial study were purchased from –Fluka- Sigma Aldrich. *E.coli* strain ATCC 35218 and *B.subtilis* strain ATCC 9372 were provided by the Microbiology lab, University of Central Florida. Hydrion paper (Fisher Scientific) was used for pH measurements. Nanopure deionized water (Barnstead) was used throughout the study.

2.2 Instrumentation

The characterization of particle size and morphology was done using JEOL JEM -1011 Transmission Electron Microscopy (TEM) and Zeiss ULTRA-55 FEG Scanning Electron Microscopy (SEM), Precision detector/Coolbatch 40T Dynamic Light Scattering (DLS) detector

was used to characterize the particle size distribution in suspension. Loading of copper was quantified by Atomic Absorption Spectroscopy (AAS) – Perkin Elmer Analyst 400 AA flame spectrometer Turbidity for antibacterial study was measured with Teysche800 spectrophotometer and the intensity of resofurin was measured on SPEX Horiba Yobin-Yvon Nanolog fluorescence spectrometer. Bacterial live/dead cell imaging was done with a ZEISS Axioskop2 confocal microscope.

2.3 Methods

2.3.1 Approach 1

2.3.1.1 Synthesis of silica nanoparticles

Stö bers silica nanoparticles (SiNP) were synthesized by addition of the reagents in the same order (1to 4) as mentioned in Table 1[23] and stirred on the magnetic stirrer for 24 hours at 400 rpm. After 24 hours, the nanoparticle solution was isolated by centrifugation at 10, 000 rpm for 10 minutes and purified by washing three times with water. The final pellet was dispersed in 100 mL water and stored at room temperature.

2.3.1.2 Synthesis of copper –loaded silica nanoparticles

The copper – loaded silica nanoparticles (CuSiNP) were synthesized following a two-step method **(Figure 1)**. The first step involved the synthesis of SiNPs by adding the reagents (1 to 4) mentioned in Table 1[23]. The reaction mixture was allowed to stir on a magnetic stirrer at 400 rpm. After 24 hours, the particles were isolated and purified with water by centrifugation at 10,000 rpm for 10 minutes. The second step involved the addition of 593.35 mg of copper sulfate to 100 mL of synthesized SiNPs to allow the formation of copper-loaded silica nanoparticles. After 4 hours of stirring on the magnetic stirrer, the CuSiNPs were washed with water by centrifugation at 10, 000 rpm for 10 minutes.

An alternate approach of synthesis of copper-loaded silica nanoparticles was also tried, where copper sulfate was added during the synthesis of silica nanoparticles **(Figure 2)**. 593.35 mg of copper sulfate was added along with the reagents mentioned in Table 1[23] and stirred magnetically at 400 rpm for 24 hours. The purification procedure as mentioned above was carried out to obtain pure CuSiNPs.

S.No	Reagent	Volume added (mL)
1	Ethanol	100
2	Water	2.97
3	Tetraethyl ortho silicate	3.78
4	Ammonium hydroxide	4.85

Table 1 - Synthesis of silica nanoparticles

2.3.2 Approach 2

2.3.2.1 Synthesis of hybrid copper –loaded silica nanoparticles

The copper – loaded silica nanoparticle synthesized in approach 1 was modified by the addition of TSPETE (N-(Trimethoxy Silyl Propyl) - Ethylenediamine, Triacetic acid, Trisodium salt 45% in water). 1.25 mL TSPETE[28] was added to the synthesized copper-loaded silica nanoparticles and stirred magnetically at 400 rpm for 4 hours. The solution separated into two parts – a top light blue solution and a bottom blue colored gel-like substance. After 4 hours, the bottom gel was separated and dissolved in 25 mL water. It was further centrifuged at 10,000 rpm for 10 minutes to remove unbound copper. The supernatant was stored separately and used for further studies.

2.3.3 Approach 3

2.3.3.1 Synthesis of "seed" silica nanoparticles

A published protocol by Rossi et al.[16] was followed for the synthesis of silica nanoparticles (SiNP). A mixture of tetraethylorthosilicate (TEOS, 1.3 mL) and ethanol (95% V/V; 5.7 mL) was added to a solution of ammonium hydroxide (28 to 30 % V/V; 7 mL), DI water (3.0 mL) and ethanol (95% V/V; 13 mL) under magnetic stirring conditions. The mixture

attained from the reaction was stirred at 400 rpm for 1 hour and sonicated for 10 minutes later. Centrifugation at 10,000 rpm for 10 minutes isolates the silica nanoparticles which were then washed with ethanol thrice for purification.

2.3.3.2 Synthesis of core-shell Cu loaded silica nanoparticles

There are two steps (Step I and Step II) in the Synthesis of core-shell Cu loaded silica nanoparticles (C-S CuSiNPs). In step I pure Stöber silica "seed" particles were synthesized using a published protocol by Rossi et al.[16]. 1.3 ml TEOS (a silane precursor for silica nanoparticle) and 5.7 mL ethanol (95% V/V) mixture were added to a solution of 13 mL ethanol (95% V/V), 7 mL ammonium hydroxide (28 to 30 % V/V) and 3 mL water under stirring conditions. The reaction mixture was stirred for an hour at 400 rpm followed by sonication for 10 minutes using a sonic bath (Barnstead Elma 9322). SiNP purification involved centrifugation and washing steps. The isolation of particles were done via centrifugation at 10,000 rpm for 10 minutes followed by repeated washings with ethanol (95%, V/V).Centrifugation and vortexing procedures were used between the two washing steps.

In step II, Cu loaded silica shell was grown on the silica "seed" particles at room temperature. In a typical procedure the "seed" particles were dispersed under magnetic stirring at 400 rpm in 75 µL of 1% hydrochloric acid (Fisher Scientific) followed by addition of 38.6 mg of copper sulfate pentahydrate in 25 mL of DI water. 650 µL of TEOS was added under stirring conditions. The Cu-silica shell growth process was allowed to continue for 24 hours. The

resulting C-S CuSiNPs were then isolated from the reaction mixture and washed thoroughly following the procedure as described above.

2.3.4 Nanoparticle characterization techniques

Sample preparation for SEM and TEM was done by spin coating the nanoparticle solution on silicon wafers and drop casting on copper grids respectively. Atomic absorption spectroscopy (AAS) analysis was done by comparison with a series of copper standards. Sample preparation involved extraction of Cu from lyophilized copper-loaded silica nanoparticle powder using saturated ethylenediaminetetraacetic acid (EDTA) solution. The EDTA leaches out Cu from the C-S CuSiNP material, forming water-soluble Cu-EDTA complex

2.3.5 Antibacterial assays

Bacterial growth inhibition test using turbidity and two standard biochemical assays (Resazurin and Baclight assays) were performed to determine antibacterial properties of copper-loaded silica nanoparticle material against a gram positive *Bacillus subtilis* (*B.subtilis*, ATCC 9372) and a gram negative *Escherichia coli* (*E.coli*, ATCC 35218) organism. A single colony was inoculated in 10 mL of the broth and grown overnight at 36^{o}C on a 150 rpm shaker. Subcultures were periodically made on LB agar plates to maintain the organisms. Kocide® 3000 (Cu hydroxide nanoparticles, represented as "insoluble" Cu compound) and copper sulfate with

same metallic copper concentration were used as positive control and silica nanoparticle (without Cu loading) was used as negative control.

2.3.5.1 Disk diffusion assay

Blank paper disks were saturated in 5 mL of the copper-loaded silica nanoparticle solution. The disks were dried in vacuum overnight. The dried disks were then placed on Mueller – Hinton agar plates already spread with bacteria. The plates were kept inverted at 36^{o}C. After 24 hours, the zone of inhibition was measured. SiNP was used as the negative control.

2.3.5.2 Bacterial growth inhibition in LB broth using turbidity

Different concentrations of copper-loaded silica nanoparticles were made in LB broth to a final volume of 10 mL. 10^5 cells/mL of the bacteria were added to all tubes. Silica ("seed") nanoparticle (without Cu loading) was taken as the negative control. Different concentrations of Kocide® 3000 and copper sulfate with same metallic concentration as in copper-loaded silica nanoparticles were considered as the positive control. Since copper-loaded silica nanoparticles, SiNP and Kocide® 3000 are turbid in nature and could interfere with the measurements of optical density; to calculate the final reading the background measurements were subtracted. All the tubes were shaken well and incubated at 36^{o}C on a 150 rpm shaker. After 24 hours, aliquots were taken to measure the optical density at 600 nm.

2.3.5.3 Minimum Inhibitory Concentration (MIC) determination

Resazurin assay method was used to determine the MIC of C-S CuSiNPs against *E.coli and B.subtilis*[29]. A 12 well cell culture plate was labeled. Different concentrations of C-S CuSiNP (2.45 to 14.7 ppm copper concentartion) were added to the wells. Silica nanoparticle was taken as the negative control. The total volume in all wells was made to 3mL with autoclaved water. 10^5 cells /mL of bacteria was added to all the wells. 150 µL of resazurin dye solution (6.75mg/mL) was then added to the wells. One well was maintained as control for resazurin (without bacteria and sample) and another well as control for the bacteria (without sample but with resazurin). The plate was sealed with parafilm and incubated on a 150 rpm shaker at 36^{o}C. Since the C-S CuSiNP was turbid in nature, intermediate colors were obtained. So the fluorescence property of resofurin was taken into account and the intensity of fluorescence was measured to find the MIC.

2.3.5.4 Bac-Light assay for live/dead cell staining

C-S CuSiNPs were incubated with 10^5 cells/mL bacteria in LB broth to determine cell viability using the BacLight bacterial viability kit L7012. 10^5 cells/mL of *E.coli* and *B.subtilis* were incubated with two different concentrations of C-S CuSiNP (9.8 and 1.4 ppm) for 4 hours on a 150 rpm shaker at 36^{o}C. Kocide® 3000 and copper sulfate at copper concentration of 9.8 ppm was considered as positive control. Silica nanoparticles (without copper) were taken as negative control. The samples were then purified from LB broth with 0.85% saline by

centrifuging at 10,000 rcf for 10 minutes. 3 µL of dye per mL of the bacterial sample was added and incubated at room temperature for 15 minutes. Images of live/dead cells were taken using a confocal microscope (Zeiss Axioskop 2). The green filter (535nm) was used to view live cells and red filter (642 nm) for dead cells[28].

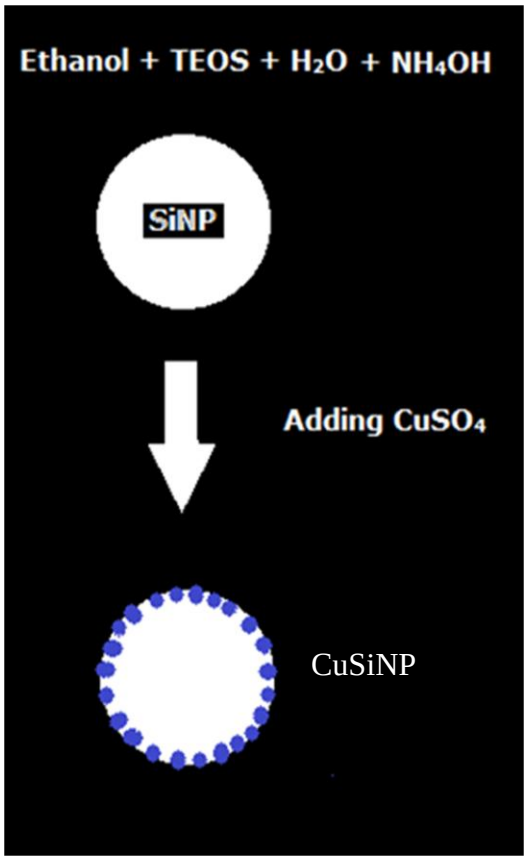

Figure 1 - Synthesis of copper-silica nanoparticles - Approach 1 (Trail 1)

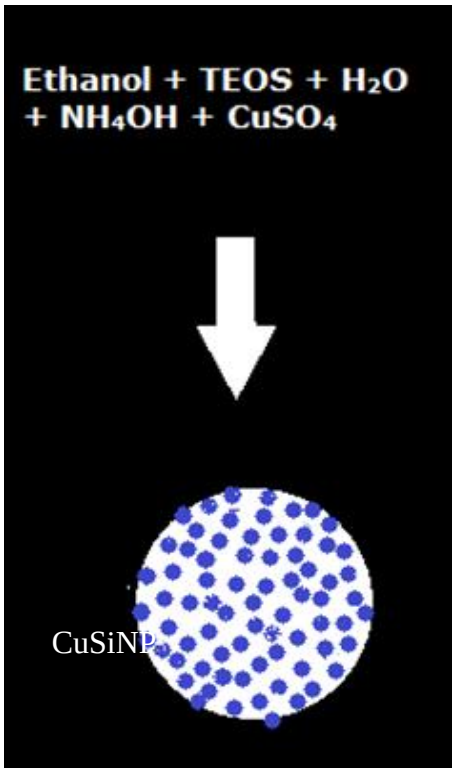

Figure 2 - Synthesis of copper-silica nanoparticles - Approach 1(Trail 2)

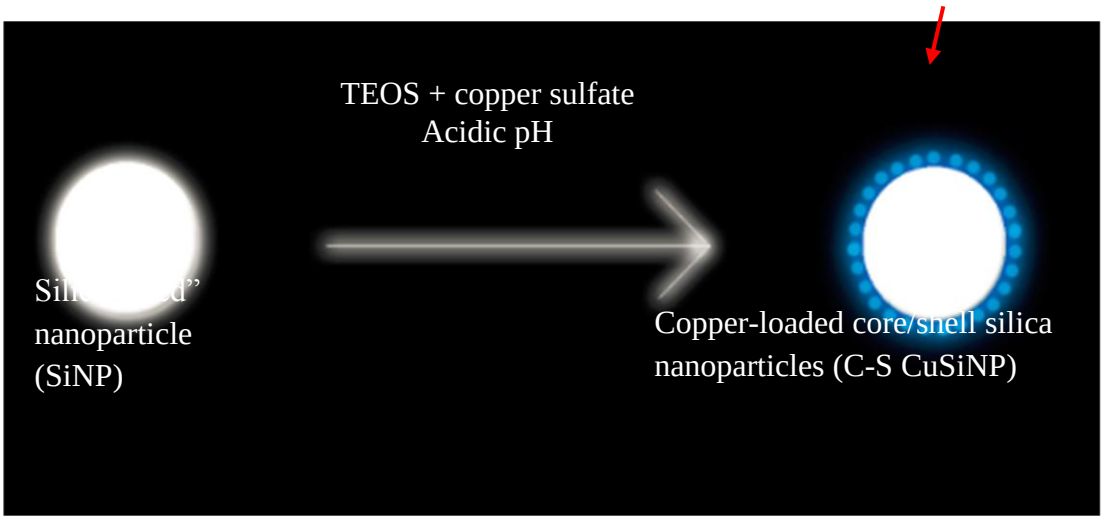

Figure 3 - Synthesis of core-shell copper loaded silica nanoparticles

CHAPTER 3 RESULTS AND DISCUSSION

3.1 Approach 1

Addition of copper sulfate to synthesized SiNP resulted in a copper retention of 0.2 ppm, while addition of copper sulfate during SiNP synthesis resulted in a copper retention of 0.4 ppm by Atomic absorption spectroscopy (AAS). Since the amount of copper retained was comparatively higher in the second trail, the CuSiNP synthesized by trail 2 was considered for further studies.

3.1.1 Nanoparticle characterization

SEM image analysis revealed the formation of highly monodispersed spherical SiNPs with smooth surface morphology (**Figure 4**). However for CuSiNPs **(Figure 5)**, particle aggregation could be seen which can be attributed to the binding of Cu ions to particle surface, resulting in reduction of overall surface charge. DLS data showed uniform particle distribution in solution. The average particle size was estimated to be 107 nm for SiNP **(Figure 6)** and 200 nm for CuSiNP **(Figure 7)** confirming with the SEM results. SEM-EDS elemental composition data showed a characteristic peak for copper, confirming the presence of copper in CuSiNP **(Figure 8)**. The amount of copper was estimated to be 0.4 ppm from atomic absorption spectroscopy (AAS).

3.1.2 Antibacterial studies

Disk diffusion assay resulted in a zone of inhibition of ~18mm **(Figure 9)** showing that copper diffused out of the nanoparticle matrix and inhibited growth of *E.coli*. Inhibition of growth at different concentrations of CuSiNP (0.04 to 2 ppm) was evaluated after 24 hours of incubation at 36^{o}C by measuring the optical density at 600nm. Significant inhibition of growth of *E.coli* was observed in the presence of CuSiNP when compared to SiNP (no copper) **(Figure 10)**. However, total inhibition could not be achieved due to less copper retention in CuSiNP (0.4 ppm copper concentration per mL of CuSiNP).

3.2 Approach 2

Copper retention in approach 1 was very less. CuSiNPs were formed as aggregates and the dispersibility was very low. To overcome these limitations, TSPETE a surface modifier[30] and copper chelator was added to synthesized CuSiNP. Few minutes after the addition of TSPETE, blue gel-like substances began to separate from the solution and stick to the sides and bottom of the container. The top solution was light-blue in color and the bottom gel-like substance was deep blue in color and water soluble. DLS analysis of both the solutions revealed the top solution had particle size in microns and the bottom-solution had particles of ~ 105nm in size. The reason for this being TSPETE is water soluble and insoluble in ethanol. So in an ethanol medium it separates from the solution chelating most of the copper and behaving as a separate substance.

The supernatant of the bottom gel-like substance in water was considered for further characterization and antibacterial study.

3.2.1 Nanoparticle characterization

Particle size and distribution in solution was estimated using DLS technique. DLS measurements estimated the average particle size to be ~ 105nm (**Figure 11)** with a polydispersity of ~0.485 suggesting the presence of aggregate which was confirmed in SEM. SEM analysis showed aggregates of CuSiNP with individual particle size of ~50 nm **(Figure 12)**. CuSiNPs as such formed aggregates, which was seen in the SEM data of approach 1. Since TSPETE was added to pre- synthesized CuSiNP, surface modification took place for the aggregates as well as individual particles. SEM-EDS elemental composition analysis showed a characteristic peak for copper **(Figure 13)** and the amount of copper was quantified to be 1.9 ppm copper concentration per mL of Copper-loaded hybrid silica nanoparticles by AAS.

3.2.2 Antibacterial studies

Disk diffusion assay gave a zone of inhibition of ~ 20 mm showing the diffusion of copper from the silica matrix **(Figure 14)**. Inhibition of growth of *E.coli* and *B.subtilis* was performed in LB broth by measuring turbidity at 600 nm after a 24 hour incubation period at 36^{o}C. As the concentration of copper increased, the growth of both *E.coli* and *B.subtilis*

decreased **(Figure 15** and **16)** when compared to the silica nanoparticle (without copper), negative control and the positive controls, Kocide® 3000 and copper sulfate at same metallic copper concentration (**Figure 17** and **18)**. Total inhibition was not achieved due to reduced copper loaded in the hybrid silica nanoparticles.

3.3 Approach 3

The copper loaded hybrid silica nanoparticles synthesized by approach 2 had its own limitations. The final solution had two products. The amount of the deep blue bottom gel increased with increase in TSPETE.

In the third approach, a totally different method of synthesis was tried involving both acid and base hydrolysis in a seeded – growth fashion. Stöber silica nanoparticles (base hydrolysis) was considered as the seed and copper-silica (acid hydrolysis) was grown as the shell around it

3.3.1 Nanoparticle characterization

The formations of highly monodispersed spherical "seed" SiNPs were noticed with smooth surface morphology **(Figure 19)** when SEM image analysis was done. The average particle size attained with this analysis was of 380 nm which on comparison to the C-S CuSiNPs particle size (estimated to be 440 nm - **Figure 20**) confirms seeded growth in the particle size of C-S CuSiNPs by ~35 nm. A more detailed investigation of the SEM image revealed that there is no separate nucleation and growth of CuSiNPs (i.e. other than "seeded" growth) confirming the

robustness of the synthesis protocol. The surface morphology of the C-S CuSiNPs was very uniform and smooth, suggesting acid-catalyzed fast hydrolysis but slow "seeded" growth process. In TEM, the shell and the core could not be differentiated because of large particle size. The entire particle appeared as dark contrast **(Figure 21** and **22)**. The increase in particle size for C-S CuSiNP when compared to SiNP core was consistent with the SEM images. The presence of copper was confirmed with the SEM-EDS compositional analysis which showed the presence of copper peak in C-S CuSiNP **(Figure 23)**. Estimation of particle size and distribution in solution was done using DLS technique. The estimations from the DLS technique showed the average particle size to be ~ 430 for SiNP (**Figure 24**) and ~ 438 for C-S CuSiNP **(Figure 25)**. The difference in particle size in DLS when compared to electron microscopy images could be attributed to the particle-particle interaction in solution. The amount of copper loading in C-S CuSiNP was quantified to be 4.9µg copper content / mL of the sample in comparison with the copper standards by AAS measurements.

3.3.2 Antibacterial studies

There was no zone of inhibition for C-S CuSiNP. This could be attributed to the large particle size (~440nm) of C-S CuSiNP, holding the copper and unable to diffuse through the agar which resulted in the inhibition of growth of bacteria through direct interaction of C-S CuSiNP.

The growth inhibitory effects of C-S CuSiNP against *E.coli* and *B.subtilis* were studied in Luria Bertani (LB) medium (**Figure 26** and **28)**. Bacterial growth at different concentrations of C-S CuSiNP (0.49 to 9.8 ppm) was evaluated after 24 hours of incubation at 36^{o}C by measuring

the optical density at 600nm (Teysche800 spectrophotometer). Significant inhibition of bacterial growth against *B.subtilis* and *E.coli* was observed due to presence of C-S CuSiNPs in growth medium. Interestingly, *B.subtilis* was more susceptible to C-S CuSiNPs than *E.coli*. This difference in susceptibility could be attributed to the difference in cell wall structure and components between the two organisms[31]. Compared to Kocide® 3000 and copper sulfate at same metallic copper concentration, C-S CuSiNP exhibited improved antibacterial efficacy against both *E.coli* and *B.subtilis* (**Figure 27** and **29).** Improved antibacterial efficacy of C-S CuSiNP is attributed to increased copper bioavailability (i.e. more "soluble" Cu).

Cu hydroxide is a water-insoluble compound (solubility product, K_{sp} is 2.2×10^{-20}) and therefore it will produce less "soluble" Cu when dispersed in water. Less "soluble" Cu means limited Cu bioavailability and hence limited anti-bacterial efficacy. Kocide® 3000 is an ultra-fine (sub-micron size) particulate Cu hydroxide compound. It is therefore expected that due to high surface area to volume ratio, Kocide® 3000 Cu hydroxide will produce more "soluble" Cu than fine (micronized) or bulk Cu hydroxide compound. However, due to inherent water-insolubility, overall Cu bioavailability of Kocide® 3000 Cu hydroxide is expected to be much less than any "soluble" Cu compound. On the other hand, copper sulfate at neutral pH gets converted to copper oxide and obtains a crystalline structure. As a result anti-bacterial efficacy of Kocide® Cu hydroxide and copper sulfate will be limited. In contrast, Cu environment in C-S CuSiNP material is very different than any "insoluble" or "soluble" Cu compounds. Cu (II) ions in C-S CuSiNP are weakly chelated by the silica matrix via silica silanol (Si-OH) groups. The Cu-silica complex remains in equilibrium with the free Cu (II) ions and can be considered as mixture of

"soluble" and "insoluble" Cu, thus improving Cu bioavailability over Kocide® 3000 Cu hydroxide and copper sulfate.

Minimum Inhibitory Concentration (MIC) of C-S CuSiNP material was determined against *E.coli* and *B.subtilis* by resazurin assay[29]. Resazurin assay is a standard cell viability assay based on the oxidation-reduction of resazurin. It is blue in color in its oxidized non-fluorescent form. However, it turns pink and exhibits strong fluorescence (λ_{max} = 603nm) upon reduction to resofurin. This reduction is carried out by oxidoreductases present in viable cells[29]. In a typical resazurin assay, 150 µL of resazurin dye (6.75 mg dye per mL of DI water) was added to 3.0 mL of bacterial broth containing about $1x10^5$ cells / mL. A series of test samples were prepared with varying concentration of C-S CuSiNPs (2.45 to 14.7 ppm) in a 12 well cell culture plate (Greiner bio-one). The microtitre plates were incubated on a 150 rpm shaker at 36^oC. The color change was noted after 24 hours. Since C-S CuSiNPs are turbid in nature, the color of the resofurin was not totally pink. Intermediate color between purple and pink could be seen at higher concentrations of copper. So it was difficult to make a fair assessment of the results by visualization. Instead, the fluorescence property of the resofurin was considered. The intensity of fluorescence was measured using a nanolog fluorescence spectrophotometer. Samples that turned pink completely gave maximum emission intensity at 603nm indicating maximum number of viable cells. For intermediate colors, there was a peak shift towards the right as well as decrease in fluorescence intensity indicating decrease in the number of viable cells. No peak was obtained at 603 nm for copper concentration greater than 4.9 ppm suggesting absence of viable cells for both *E.coli* and *B.subtilis* **(Figure 30** and **31)**. Hence the MIC of C-S CuSiNP against *E.coli* and *B.Subtilis* was estimated to be 4.9 ppm copper concentration.

Baclight live/dead cell staining[28] was also done to determine the cell viability of *E.coli* and *B.subtilis.* The kit contains two dyes – propidium iodide, the red-fluorescent dye which stains damaged or deformed cells and SYTO®9, the green-fluorescent dye which stains all types of cells. However, propidium iodide is dominant in dead cells giving it the red color. The C-S CuSiNP with 9.8 ppm copper concentration showed no live cells of both *E.coli* and *B.subtilis* (**Figure 32)** indicating 99.9% inhibition consistent with the inhibition in liquid media results. C-S CuSiNP at a lower concentration (1.2 ppm copper concentration) showed more number of live (green) cells (**Figure 33).** Kocide® 3000 and copper sulfate with 9.8 ppm copper concentration showed more number of live (green) *E.coli* and *B.subtilis* cells **(Figure 34).** Silica nanoparticles (without copper) also showed more live cells **(Figure 35).** This confirms the efficient antibacterial activity of copper in C-S CuSiNP even after a short incubation time.

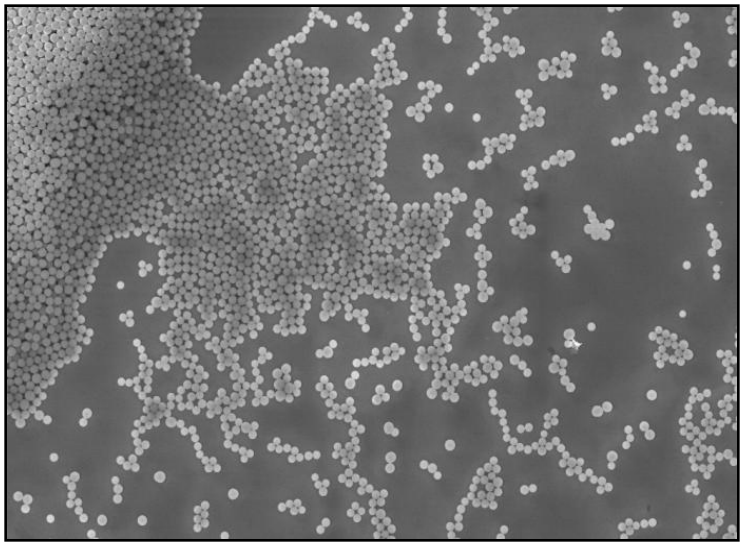

Figure 4 - Monodiserpersed spherical SiNPs with smooth surface morphology from SEM

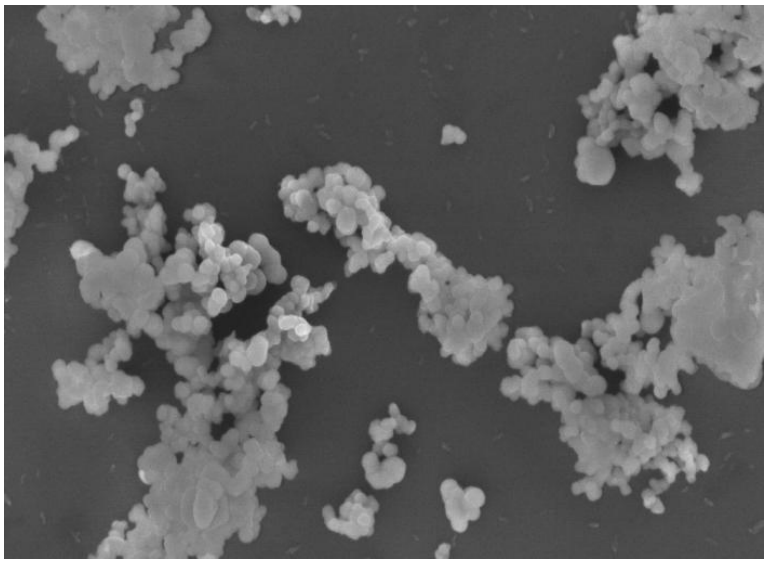

Figure 5 - Aggregates of CuSiNP from SEM

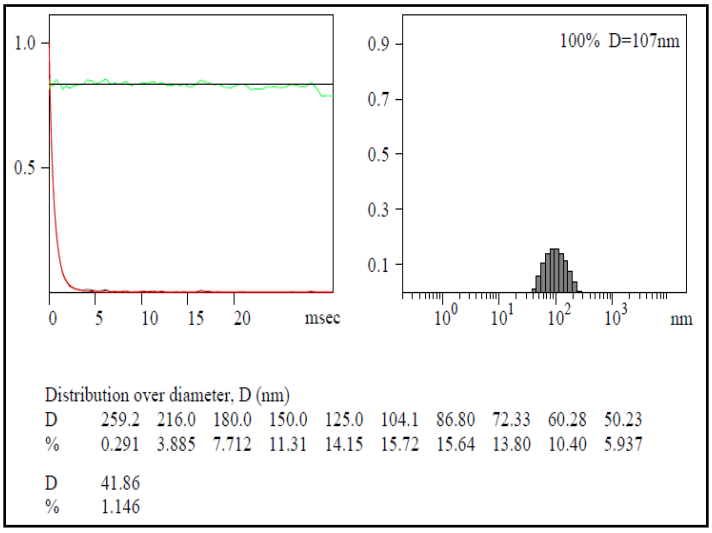

Figure 6 - SiNP distribution in water and hydrodynamic radius

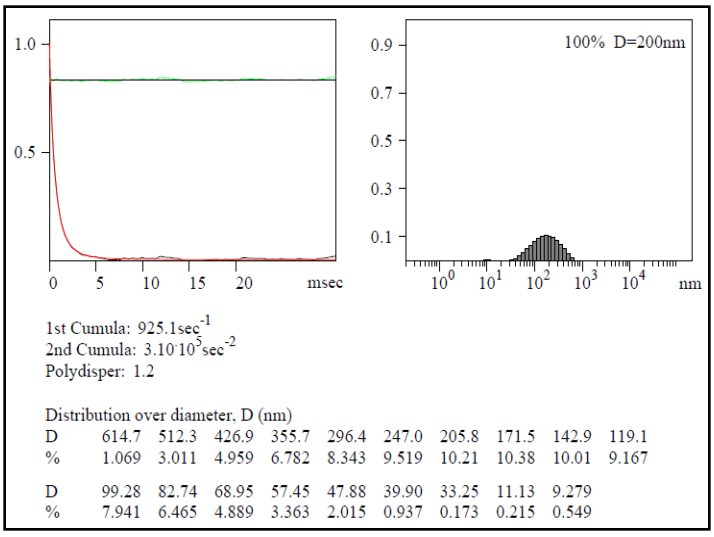

Figure 7 - CuSiNP distribution in water and hydrodynamic radius

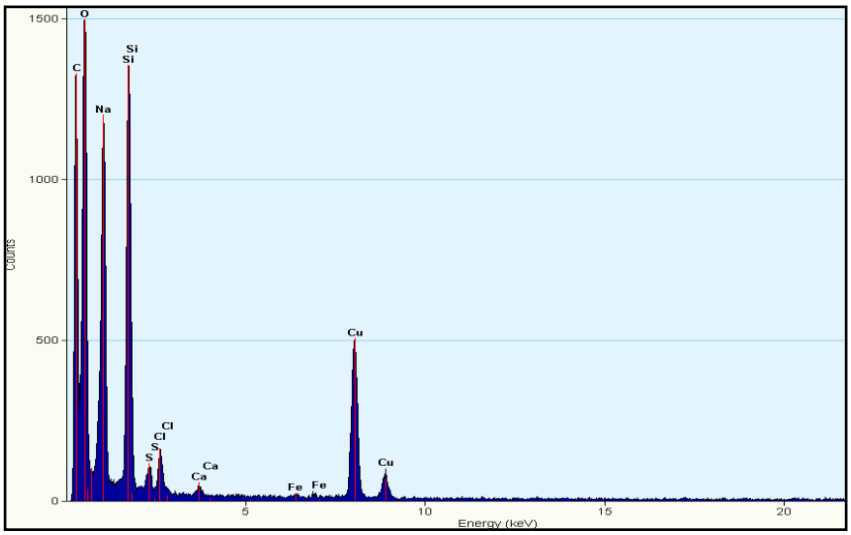

Figure 8 - SEM - EDS elemental composition of CuSiNP showing a characteristic peak for copper

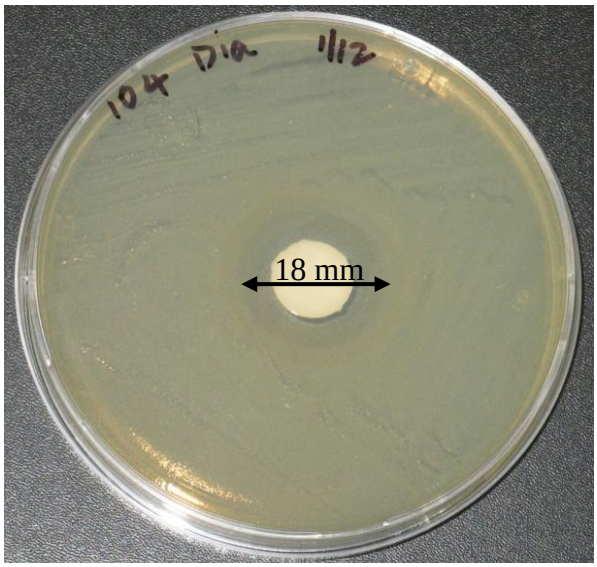

Figure 9 - Zone of inhibition of ~18 mm by copper-loaded hybrid silica nanoparticles against *E.coli*

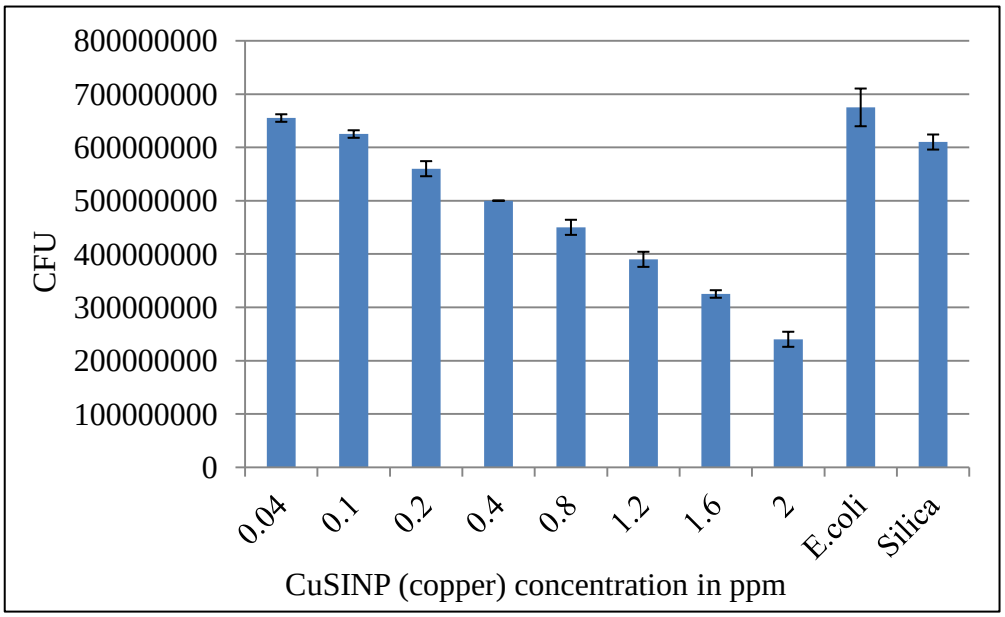

Figure 10 - Histogram showing decrease in growth of *E.coli* with increase in CuSiNP

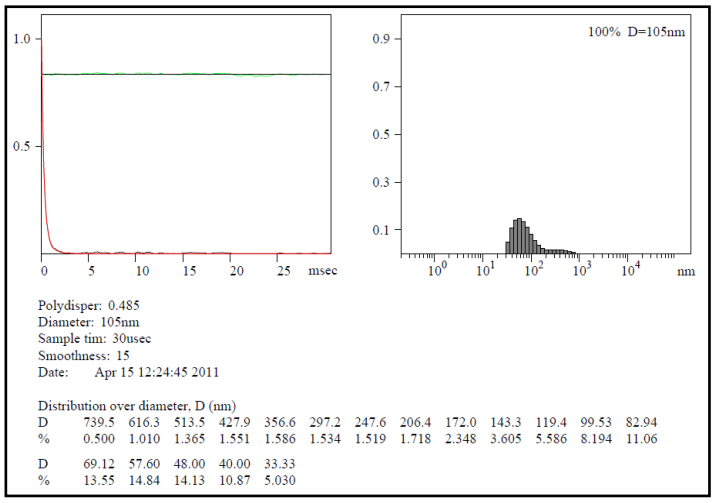

Figure 11 - Particle distribution and hydrodynamic radius of copper-loaded hybrid silica nanoparticles

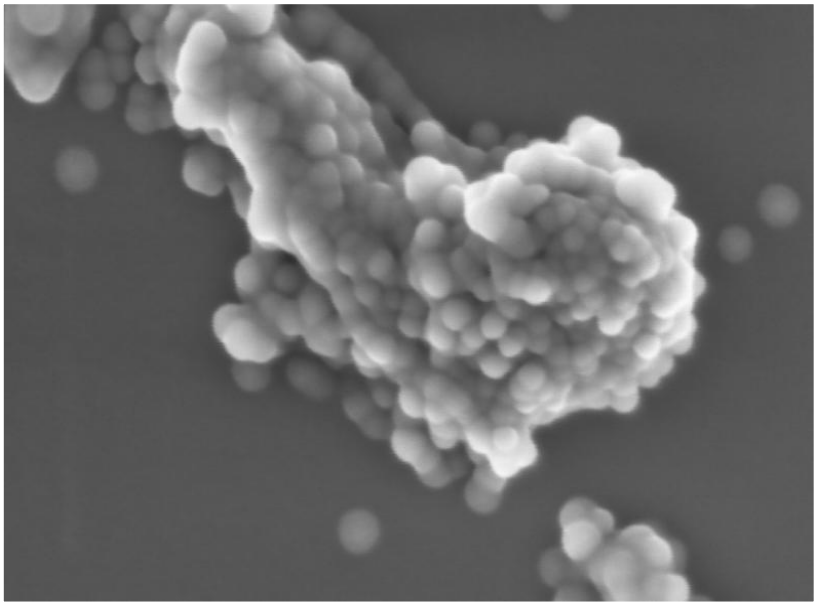

Figure 12 - Aggregates of copper-loaded hybrid silica nanoparticles from SEM

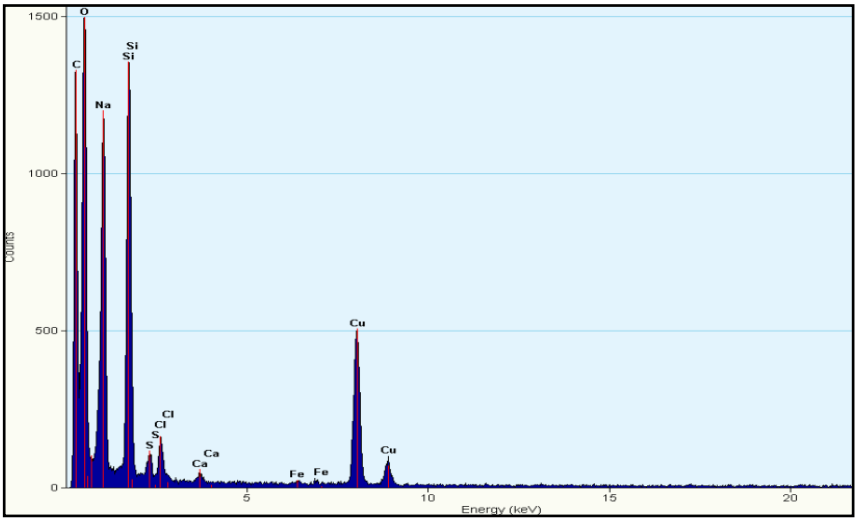

Figure 13 - Characterisctic copper peak for copper-loaded hybrid silica nanoparticles in SEM -EDS

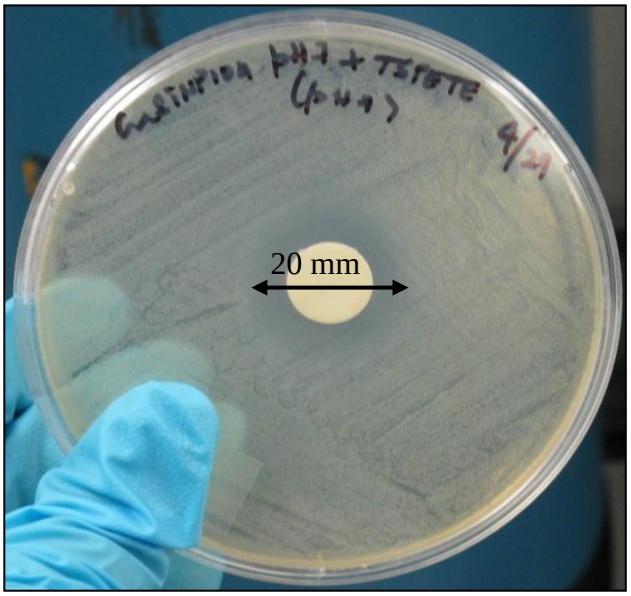

Figure 14 - Clear zone of inhibition of ~ 20mm by copper-loaded hybrid silica nanoaprticles against *E.coli*

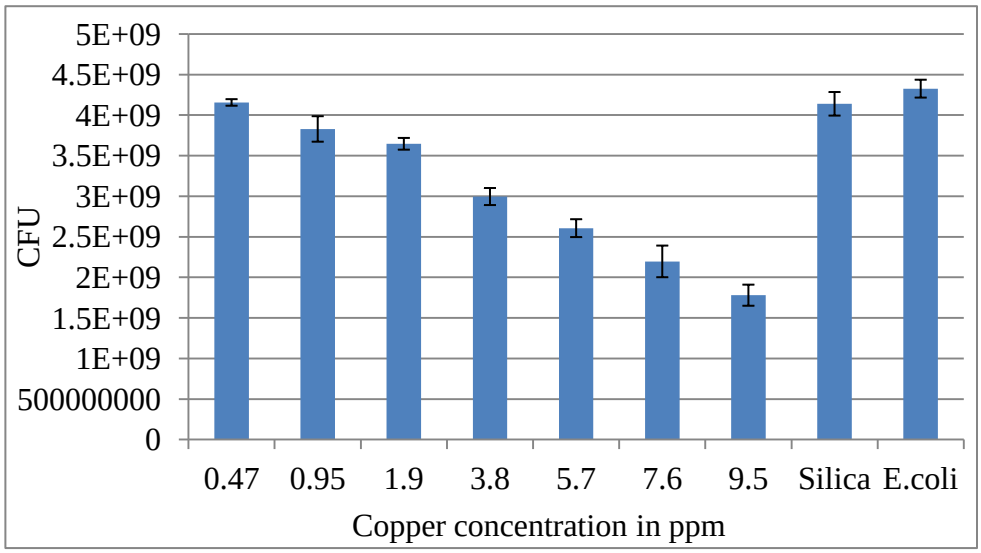

Figure 15 - Histogram showing inhibition of *E.coli* with increase in copper-loaded hybrid silica nanoparticles

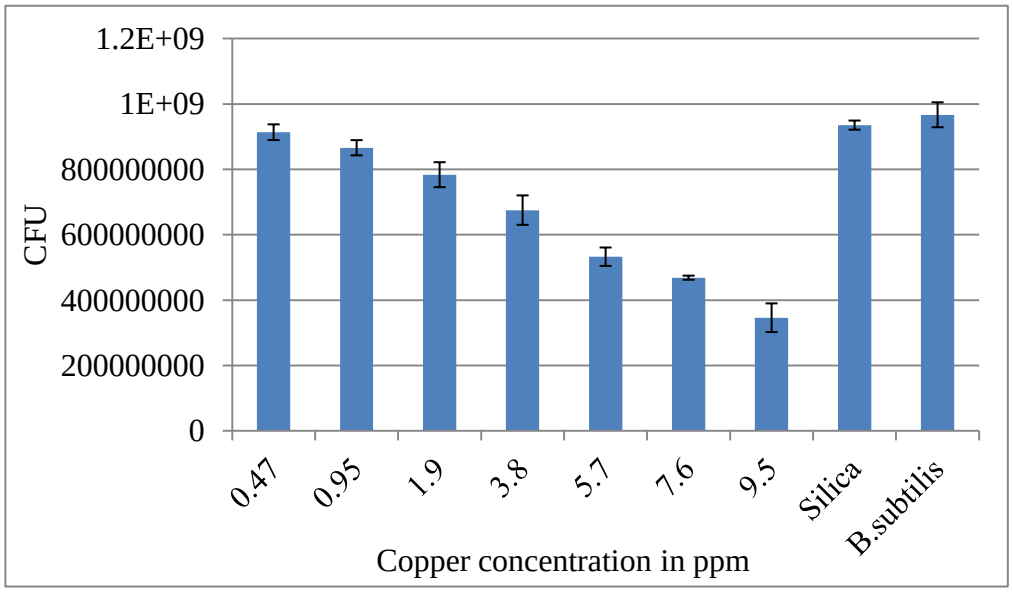

Figure 16 - Histogram showing inhibition of *B.subtilis* with increase in copper-loaded hybrid silica nanoparticles

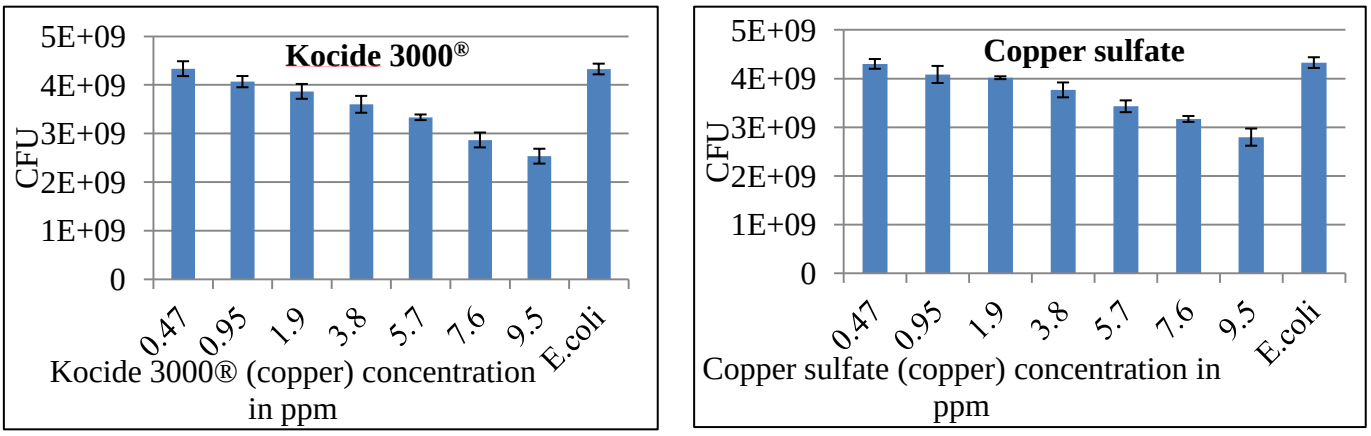

Figure 17 - Histogram showing inhibition of *E.coli* by Kocide 3000® and Copper sulfate

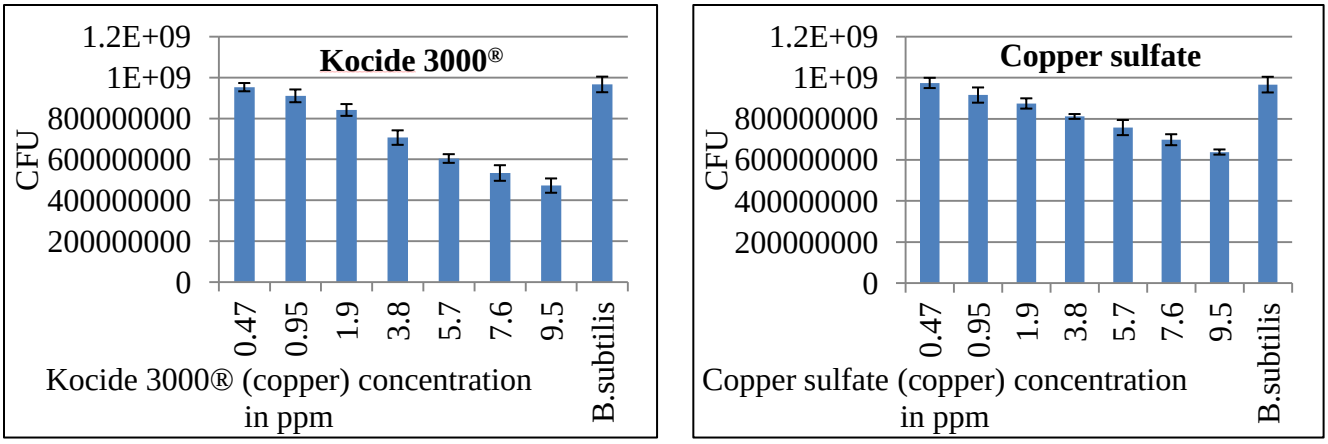

Figure 18 - Histogram showing inhibition of *B.subtilis* by Kocide 3000® and Copper sulfate

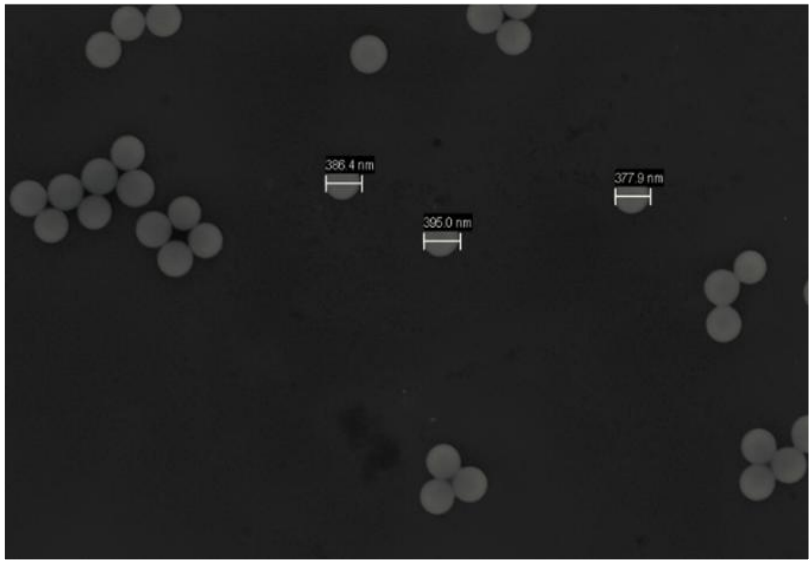

Figure 19 - Monodispersed spherical "core" SiNPs with smooth surface morphology

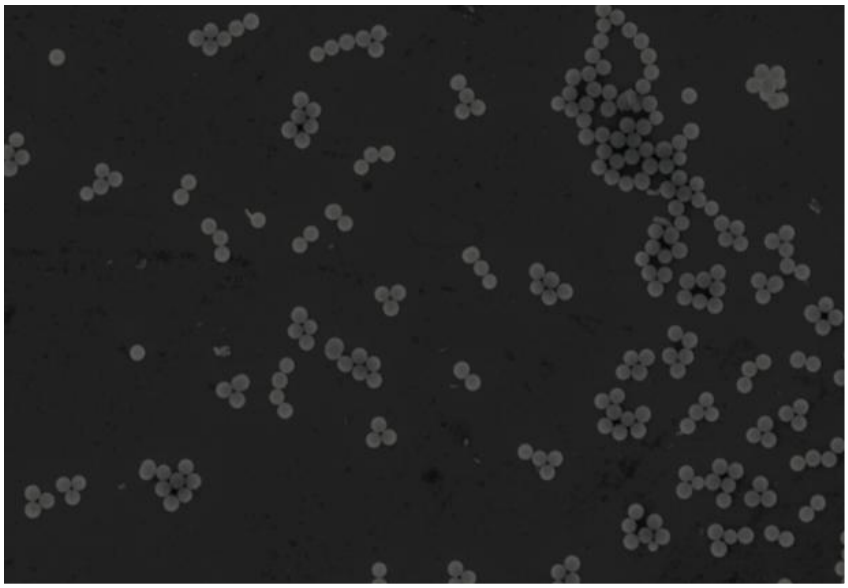

Figure 20 - Monodispersed spherical C-S CuSiNPs with smooth surface morphology

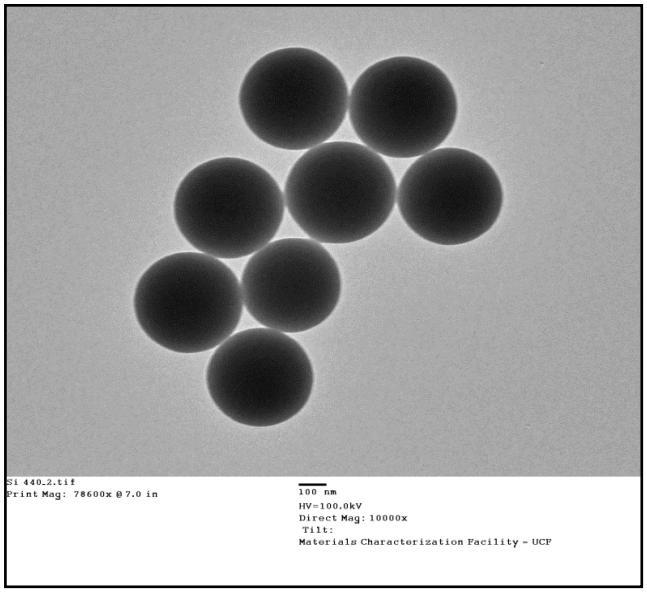

Figure 21 - Spherical "core" SiNPs image from TEM

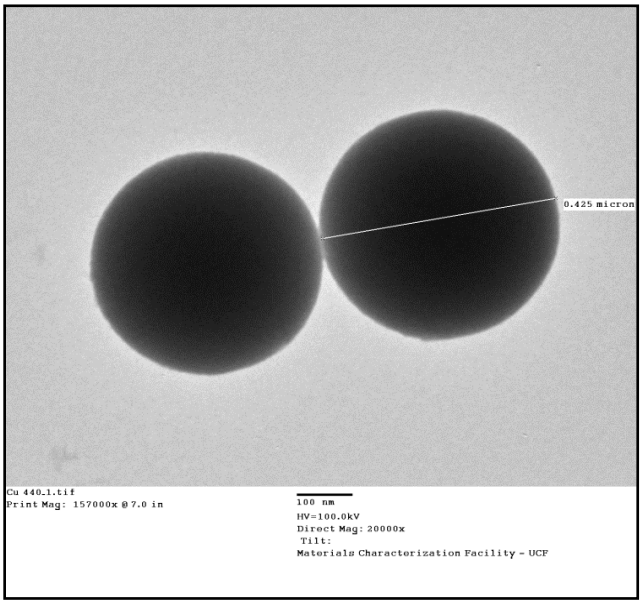

Figure 22 - Spherical shaped C-S CuSiNP with increased particle size from TEM

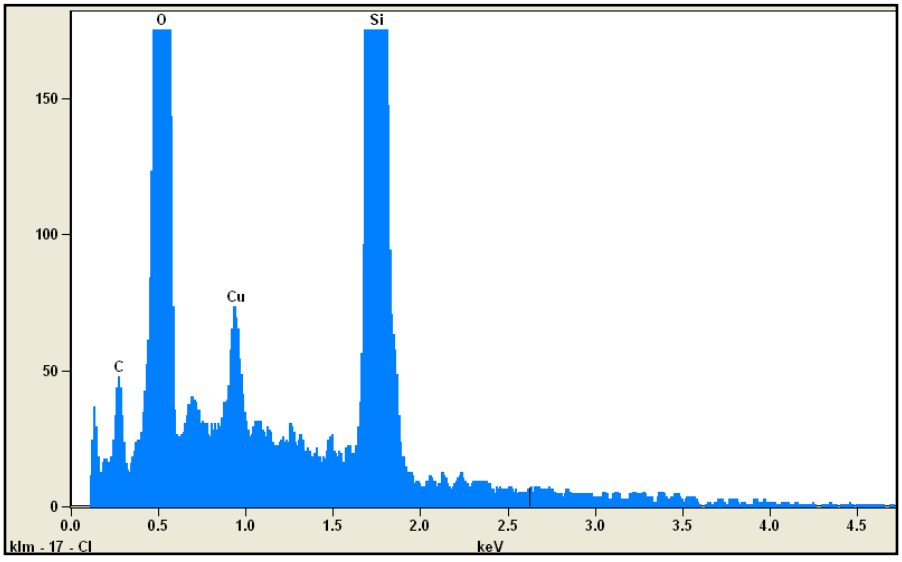

Figure 23 - Characteristic copper peak from SEM-EDS for C-S CuSiNP

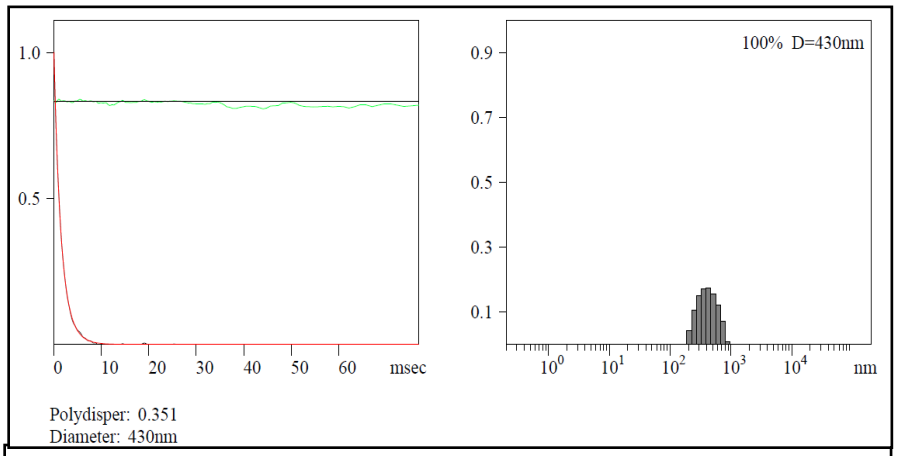

Distribution over diameter, D (nm)

D	889.4	741.1	617.6	514.7	428.9	357.4	297.8	248.2	206.8
%	0.746	7.083	12.13	15.61	17.33	17.14	14.94	10.66	4.368

Figure 24 - "Core" SiNP distribution profile and hydrodynamic radius in water

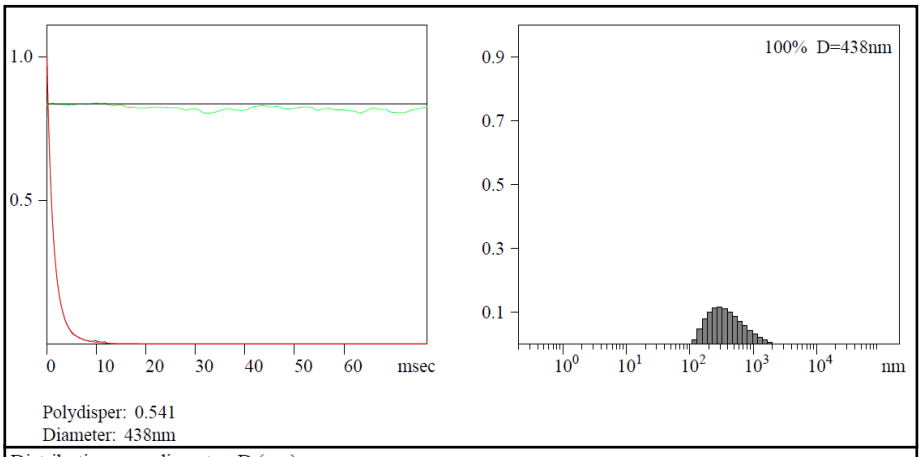

Distribution over diameter, D (nm)

D	1844	1536	1280	1067	889.4	741.1	617.6	514.7	428.9	357.4	297.8	248.2	206.8
%	0.408	1.151	2.023	3.049	4.244	5.603	7.089	8.613	10.02	11.10	11.61	11.30	10.04
D	172.3	143.6	119.7										
%	7.796	4.747	1.208										

Figure 25 - C-S CuSiNP distribution profile and hydrodynamic radius in water

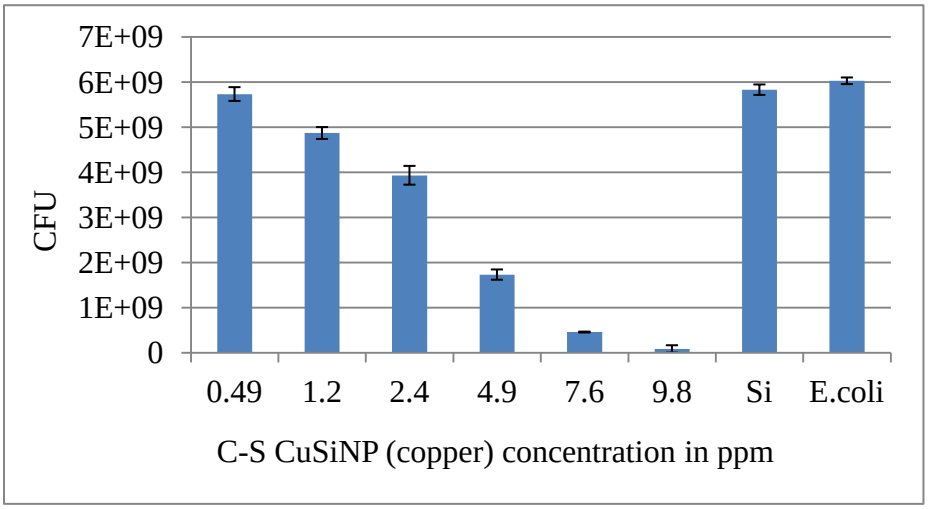

Figure 26 - Histogram showing decrease in growth of *E.coli* with increase in C-SCuSiNP

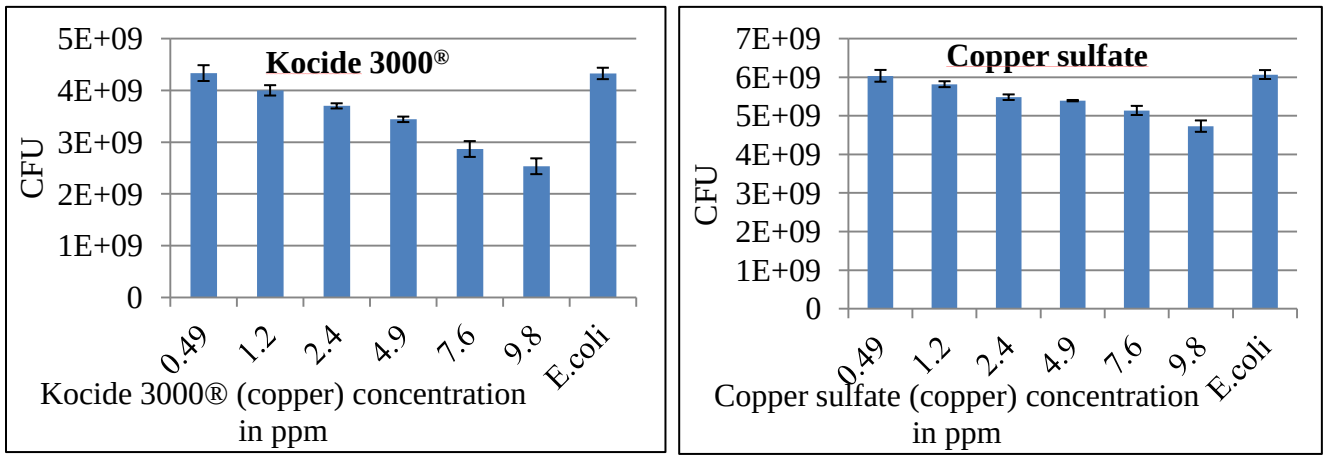

Figure 27 - Histogram showing inhibition of E.coli by Kocide 3000® and Copper sulfate

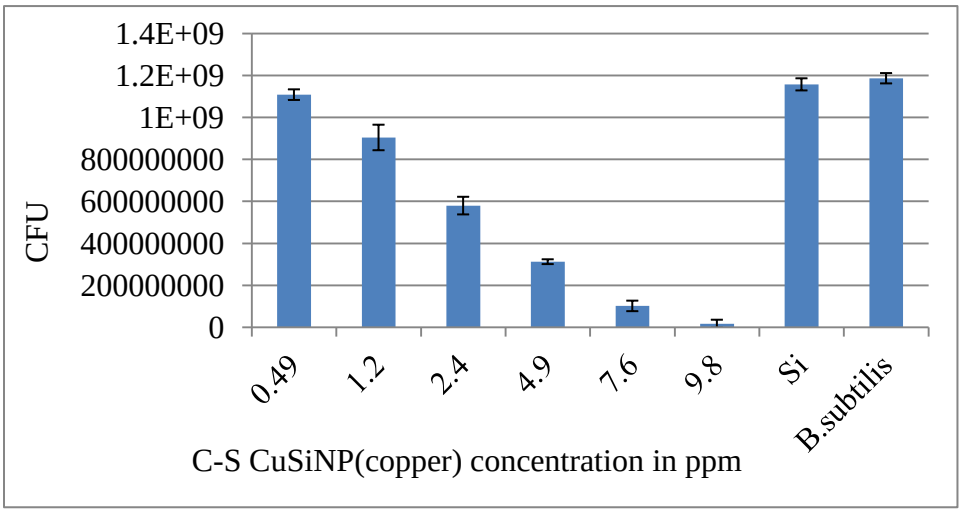

Figure 28 - Histogram showing decrease in growth of *B.subtilis* with increase in C-SCuSiNP

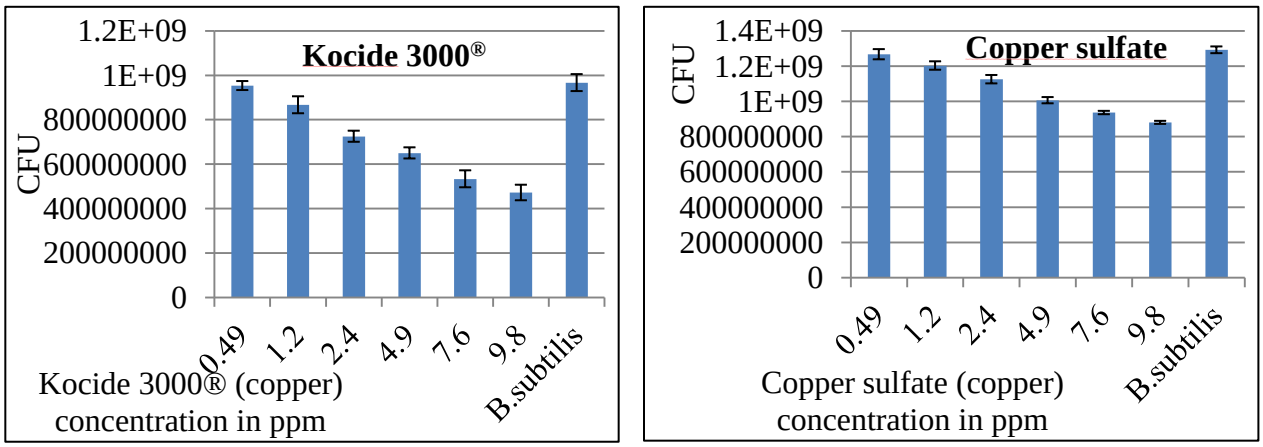

Figure 29 - Histogram showing inhibition of *B.subtilis* by Kocide 3000® and Copper sulfate

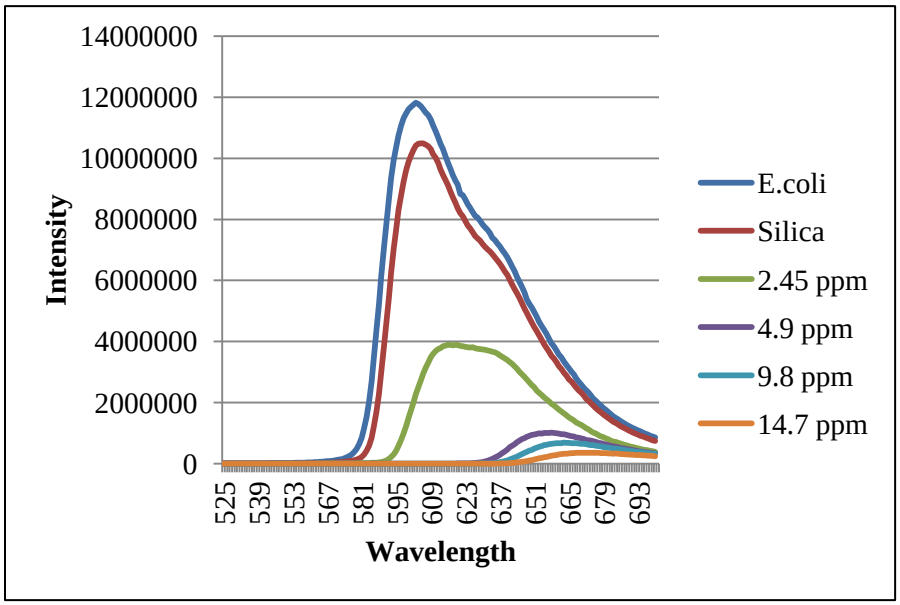

Figure 30 - Fluorescence intensity of resorufin decreases with increase in C-SCuSiNP showing decrease in viable *E.coli* cells

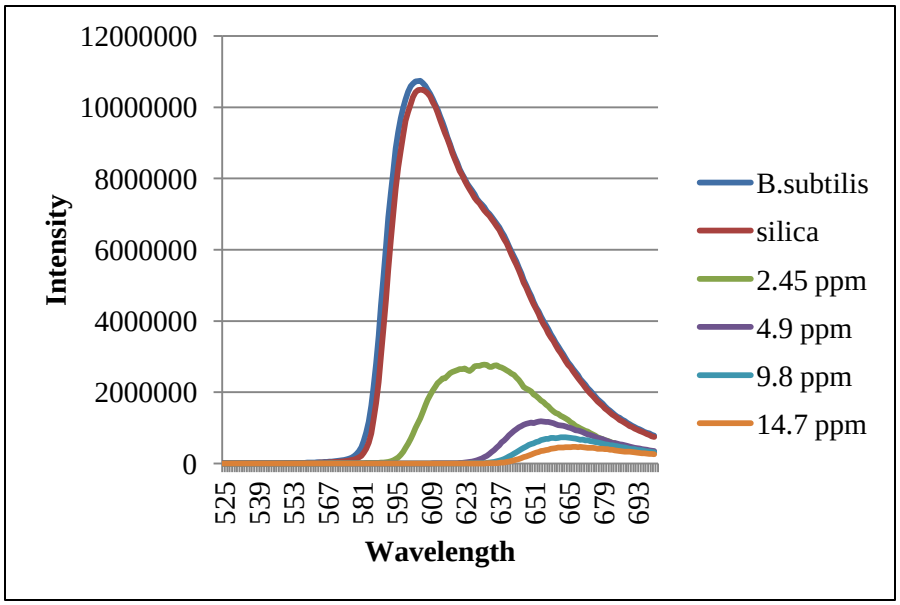

Figure 31 - Fluorescence intensity of resorufin decreases with increase in C-SCuSiNP showing decrease in viable *B.subtilis* cells

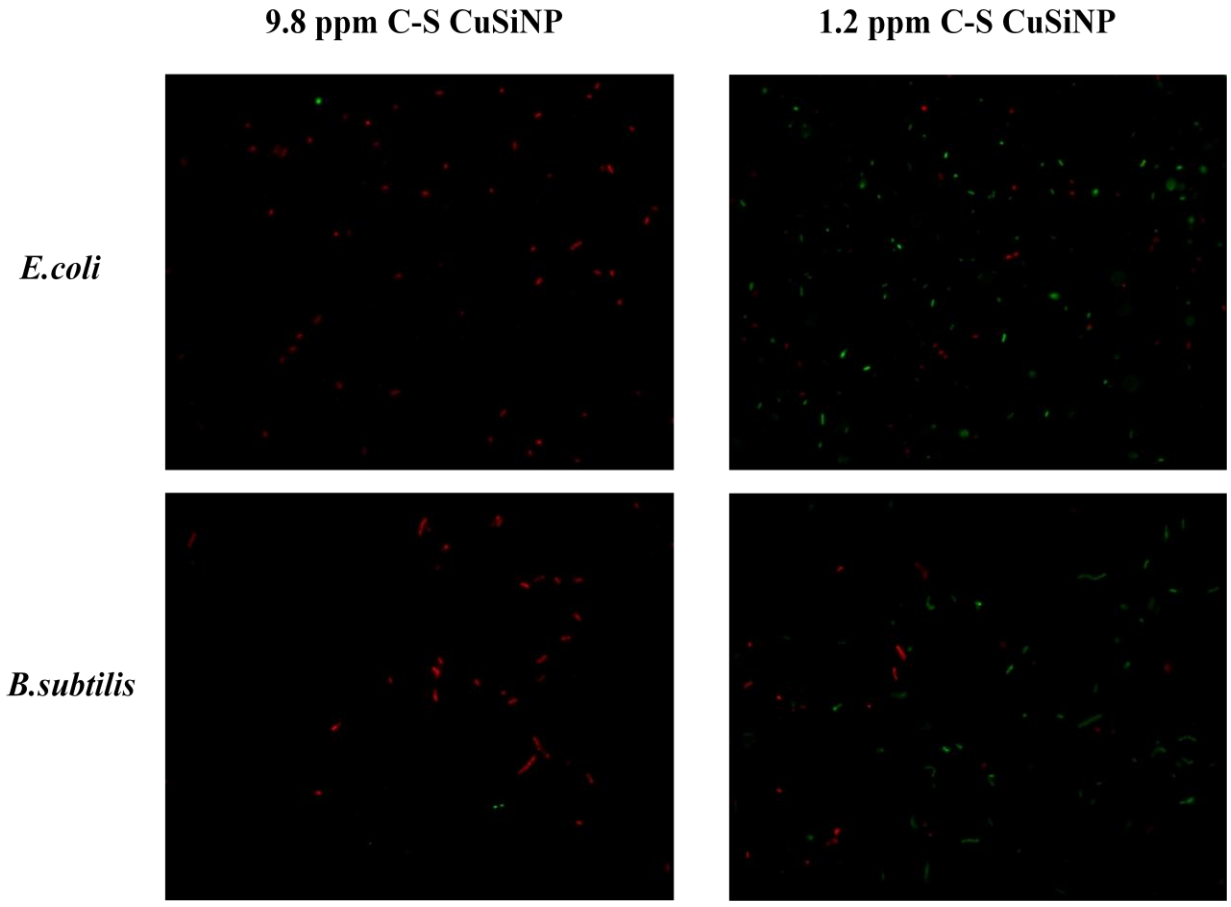

Figure 32 - Fluorescent microscopy images of *E.coli* and *B.subtilis* treated with different copper concentrations of C-S CuSiNP showing live/dead cells

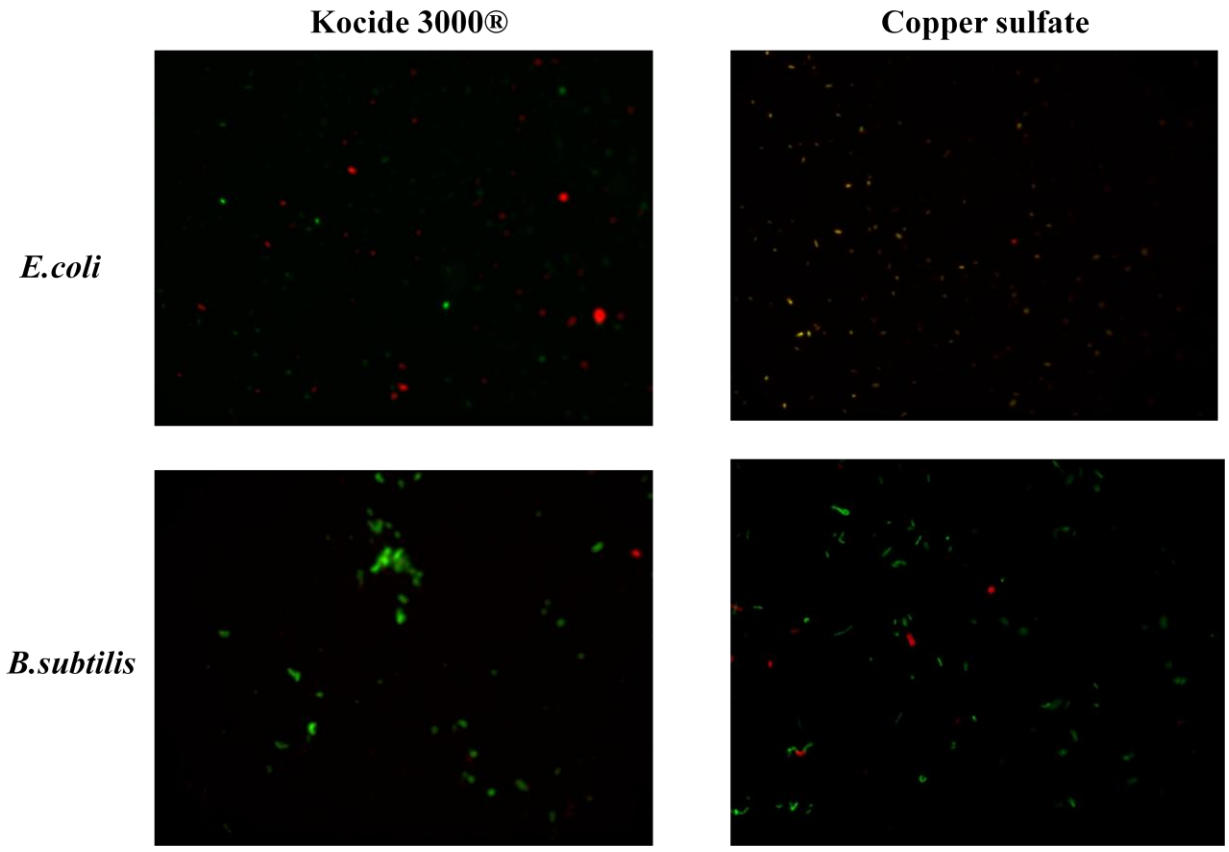

Figure 33 - Fluorescent microscopy images of *E.coli* and *B.subtilis* treated with Kocide 3000® and copper sulfate at 9.8 ppm copper concentration showing live/dead cells

E.coli

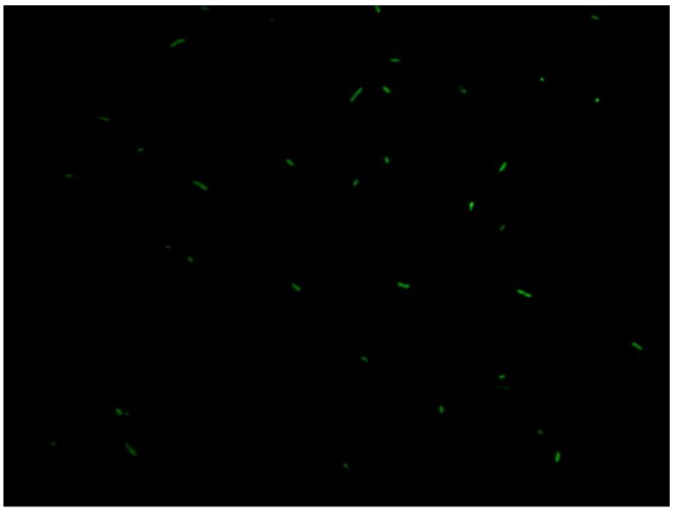

B.subtilis

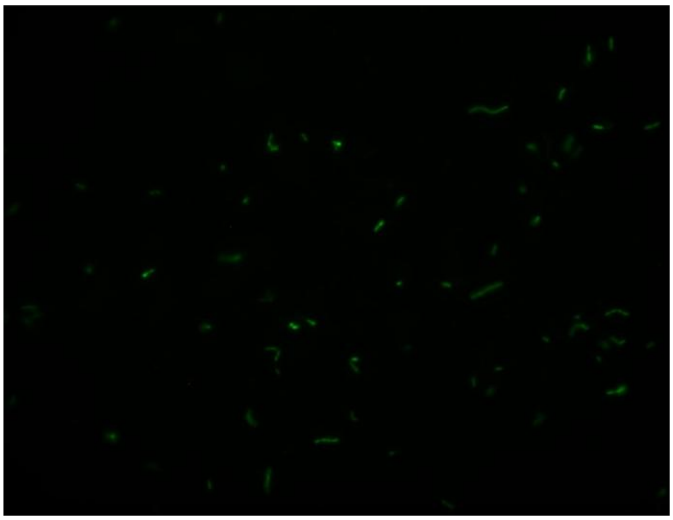

Figure 34 - Fluorescent microscopy images of *E.coli* and *B.subtilis* treated with silica nanoparticles showing live/dead cells

CHAPTER 4 CONCLUSION

Copper-loaded silica nanoparticles were synthesized in three different approaches. Each approach had its own advantages and limitations. In the first approach, a one-step synthesis of addition of copper sulfate to pre-synthesized spherical silica nanoparticles was tried. Silica NP surface is negatively charged due to deprotonation of the silanol groups at the neutral pH condition and the Cu ion in copper sulfate is positively charged. The attraction between the two oppositely charged species facilitate loading of copper on the surface of silica nanoparticles. Cu retention in the resulting CuSiNPs was insignificant (0.2 ppm) as most of the Cu ions were loaded to the silica NP surface. These CuSiNPs were highly aggregated in water. This is due to the reduction of the overall surface charge of the silica NPs after binding to Cu ions.

So in approach 2, the surface of silica nanoparticles was modified with a water-soluble silane based surface functionalizing agent, TSPETE which also served as a chelating agent for the Cu ions, forming copper-loaded hybrid silica nanoparticles. Addition of the TSPETE is expected to improve overall nanoparticle dispersibility in water as well as copper loading. The synthesis however led to the formation of two separate layers due to phase separation. A light blue top solution and a water soluble gel-like substance stuck to the bottom of the container. The top solution had particle size in microns while the bottom part had particle size ~ 50 nm. The bottom gel-like substance also had appreciable copper retention when compared to the top solution and copper-loaded silica nanoparticles of approach 1. The amount of the bottom gel-like substance increased with increase in TSPETE. This approach is not robust as it did not yield a

single product. Moreover, TSPETE is a costly chemical and therefore bulk production of the materials in a cost effective way may not be quite practical for potential agricultural applications.

Approach 3 overcomes some of the limitations of the first two approaches. It is a novel core-shell design of copper-loaded silica nanoparticles (C-S CuSiNP). This method involves both acid and base hydrolysis procedures. Stöber silica nanoparticles (synthesized by base hydrolysis) serve as the core and copper-silica (synthesized by acid hydrolysis) was allowed to grow as the shell around the silica core. Highly monodispersed, spherical shaped particles were obtained as confirmed by the SEM and TEM imaging techniques. Particle agglomeration was not seen in silica "core" nanoparticles as well as core-shell copper loaded silica nanoparticles. Improved copper loading was seen which was confirmed by the AAS. The SEM-EDS elemental composition data showed a characteristic peak for copper. Antimicrobial studies show significant growth inhibition against both gram-negative and gram-positive bacteria. Total inhibition was also achieved which can be correlated to improved copper retention. Our study indicates that bioavailability of Cu has increased in C-S CuSiNP in comparison to positive control Cu hydroxide, an "insoluble" sub-micron size Cu compound and copper sulfate due to availability of more "soluble" Cu. Improving efficacy of Cu biocide has clear advantage of reducing undesirable burden related to Cu toxicity in the environment.

For example, with improved Cu bioavailability, it is feasible to use the present C-S CuSiNPs in spray-based formulations to spray-coat touch surfaces to generate antimicrobial "touch-safe" surface. Since silica is a biocompatible material carrying only 0.01 wt% metallic Cu, it is expected that the spray formulation containing C-S CuSiNPs could be considered as environment-friendly. This design can also be used to load any other antibacterial agent (such as

silver, zinc ions, nanoparticles, antibiotics etc.) within the silica shell. The core is a biocompatible matrix and its surface can be modified easily to attach ligands.

REFERENCES

1. Borkow G, Gabbay J. Copper as a Biocidal Tool. *Current Medicinal Chemistry.* 2005;12(18):2163-2175.

2. Appendini P, Hotchkiss JH. Review of antimicrobial food packaging. *Innovative Food Science & Emerging Technologies.* 2002;3(2):113-126.

3. Freeman MH, McIntyre CR. A Comprehensive Review of Copper-Based Wood Preservatives. *Forest Products Journal.* Nov 2008;58(11):6-27.

4. Schultz TP, Nicholas DD, Preston AF. Perspective - A brief review of the past, present and future of wood preservation. *Pest Management Science.* Aug 2007;63(8):784-788.

5. Terlizzi A, Fraschetti S, Gianguzza P, Faimali M, Boero F. Environmental impact of antifouling technologies: state of the art and perspectives. *Aquatic Conservation-Marine and Freshwater Ecosystems.* Jul-Aug 2001;11(4):311-317.

6. Casey AL, Adams D, Karpanen TJ, et al. Role of copper in reducing hospital environment contamination. *Journal of Hospital Infection.* Jan 2010;74(1):72-77.

7. Gant VA, Wren MWD, Rollins MSM, Jeanes A, Hickok SS, Hall TJ. Three novel highly charged copper-based biocides: safety and efficacy against healthcare-associated organisms. *Journal of Antimicrobial Chemotherapy.* August 1, 2007 2007;60(2):294-299.

8. Voulvoulis N, Scrimshaw MD, Lester JN. Alternative antifouling biocides. *Applied Organometallic Chemistry.* Mar 1999;13(3):135-143.

9. Weaver L, Noyce JO, Michels HT, Keevil CW. Potential action of copper surfaces on meticillin-resistant Staphylococcus aureus. *Journal of Applied Microbiology.* Dec 2010;109(6):2200-2205.

10. Pavlovic M. A REVIEW OF AGRIBUSINESS COPPER USE EFFECTS ON ENVIRONMENT. *Bulgarian Journal of Agricultural Science.* Aug 2011;17(4):491-500.

11. Behlau F, Belasque J, Jr., Graham JH, Leite RP, Jr. Effect of frequency of copper applications on control of citrus canker and the yield of young bearing sweet orange trees. *Crop Protection.* Mar 2010;29(3):300-305.

12. Dafforn KA, Lewis JA, Johnston EL. Antifouling strategies: History and regulation, ecological impacts and mitigation. *Marine Pollution Bulletin.* Mar 2011;62(3):453-465.

13. Konstantinou IK, Albanis TA. Worldwide occurrence and effects of antifouling paint booster biocides in the aquatic environment: a review. *Environment International.* Apr 2004;30(2):235-248.

14. Thomas KV, Brooks S. The environmental fate and effects of antifouling paint biocides. *Biofouling.* 2010 2010;26(1):73-88.

15. Tan W, Wang K, He X, et al. Bionanotechnology based on silica nanoparticles. *Medicinal Research Reviews.* 2004;24(5):621-638.

16. Rossi LM, Shi LF, Quina FH, Rosenzweig Z. Stober synthesis of monodispersed luminescent silica nanoparticles for bioanalytical assays. *Langmuir.* May 10 2005;21(10):4277-4280.

17. Santra S. Fluorescent Silica Nanoparticles for Cancer Imaging. Vol 6242010:151-162.

18. Finnie KS, Bartlett JR, Barbé CJA, Kong L. Formation of Silica Nanoparticles in Microemulsions. *Langmuir*. 2007/03/01 2007;23(6):3017-3024.

19. Darbandi M, Thomann R, Nann T. Single Quantum Dots in Silica Spheres by Microemulsion Synthesis. *Chemistry of Materials.* 2005/11/01 2005;17(23):5720-5725.

20. Wong YJ, Zhu L, Teo WS, et al. Revisiting the Sto□ber Method: Inhomogeneity in Silica Shells. *Journal of the American Chemical Society.* 2011/08/03 2011;133(30):11422-11425.

21. Kobayashi Y, Katakami H, Mine E, Nagao D, Konno M, Liz-Marzán LM. Silica coating of silver nanoparticles using a modified Stöber method. *Journal of Colloid and Interface Science.* 2005;283(2):392-396.

22. Costa CAR, Leite CAP, Galembeck F. Size Dependence of Stöber Silica Nanoparticle Microchemistry. *The Journal of Physical Chemistry B.* 2003/05/01 2003;107(20):4747-4755.

23. Thomassen LCJ, Aerts A, Rabolli V, et al. Synthesis and Characterization of Stable Monodisperse Silica Nanoparticle Sols for in Vitro Cytotoxicity Testing. *Langmuir.* 2010/01/05 2009;26(1):328-335.

24. Ren G, Hu D, Cheng EWC, Vargas-Reus MA, Reip P, Allaker RP. Characterisation of copper oxide nanoparticles for antimicrobial applications. *International journal of antimicrobial agents.* 2009;33(6):587-590.

25. Cioffi N, Torsi L, Ditaranto N, et al. Copper Nanoparticle/Polymer Composites with Antifungal and Bacteriostatic Properties. *Chemistry of Materials.* 2011/09/25 2005;17(21):5255-5262.

26. Kim YH, Lee DK, Cha HG, Kim CW, Kang YC, Kang YS. Preparation and Characterization of the Antibacterial Cu Nanoparticle Formed on the Surface of SiO2 Nanoparticles. *The Journal of Physical Chemistry B.* 2011/09/25 2006;110(49):24923-24928.

27. Anyaogu KC, Fedorov AV, Neckers DC. Synthesis, Characterization, and Antifouling Potential of Functionalized Copper Nanoparticles. *Langmuir.* 2011/09/25 2008;24(8):4340-4346.

28. Rastogi SK, Rutledge VJ, Gibson C, Newcombe DA, Branen JR, Branen AL. Ag colloids and Ag clusters over EDAPTMS-coated silica nanoparticles: synthesis, characterization, and antibacterial activity against Escherichia coli. *Nanomedicine: Nanotechnology, Biology and Medicine.* 2011;7(3):305-314.

29. Sarker SD, Nahar L, Kumarasamy Y. Microtitre plate-based antibacterial assay incorporating resazurin as an indicator of cell growth, and its application in the in vitro antibacterial screening of phytochemicals. *Methods.* Aug 2007;42(4):321-324.

30. Yang H, Santra S, Walter GA, Holloway PH. GdIII-Functionalized Fluorescent Quantum Dots as Multimodal Imaging Probes. *Advanced Materials.* 2006;18(21):2890-2894.

31. Raffi M, Mehrwan S, Bhatti T, et al. Investigations into the antibacterial behavior of copper nanoparticles against <i>Escherichia coli</i&gt. *Annals of Microbiology.* 2010;60(1):75-80.

Additional References

1. Appendini P, Hotchkiss JH. Review of antimicrobial food packaging. *Innovative Food Science & Emerging Technologies.* 2002;3(2):113-126.

2. Flemming CA, Trevors JT. Copper toxicity and chemistry in the environment: a review. *Water, Air, & Soil Pollution.* 1989;44(1):143-158.

3. Freedman JH. The role of glutathione in copper metabolism and toxicity. *The Journal of biological chemistry.* 1989;264(10):5598-5605.

4. Fu W, Yang H, Hari B, Liu S, Li M, Zou G. Preparation and characteristics of core-shell structure cobalt/silica nanoparticles. *Materials Chemistry and Physics.* 2006;100(2-3):246-250.

5. Grass G, Rensing C, Solioz M. Metallic Copper as an Antimicrobial Surface. *Applied and Environmental Microbiology.* Mar 2011;77(5):1541-1547.

6. Hall TJ, Jeanes A, Coen PG, Odunaike A, Hickok SS, Gant VA. A hospital cleaning study using microfibre and a novel copper biocide. I. Microbiological studies. *Journal of Infection Prevention.* September 1, 2011 2011;12(5):188-194.

7. Han B-H, Antonietti M. One-step synthesis of copper nanoparticles containing mesoporous silica by nanocasting of binuclear copper(ii) complexes with cyclodextrins. *Journal of Materials Chemistry.* 2003;13(7):1793-1796.

8. Liong M, France B, Bradley KA, Zink JI. Antimicrobial Activity of Silver Nanocrystals Encapsulated in Mesoporous Silica Nanoparticles. *Advanced Materials.* May 4 2009;21(17):1684-+.

9. Lossin A, Westhoff F-J. The production and application of cuprous oxide and cupric hydroxide. *JOM Journal of the Minerals, Metals and Materials Society.* 1997;49(10):38-39.

10. Luna VA, Hall TJ, King DS, Cannons AC. Susceptibility of 169 USA300 methicillin-resistant Staphylococcus aureus isolates to two copper-based biocides, CuAL42 and CuWB50. *Journal of Antimicrobial Chemotherapy.* May 1, 2010 2010;65(5):939-941.

11. Mikolay A, Huggett S, Tikana L, Grass G, Braun J, Nies DH. Survival of bacteria on metallic copper surfaces in a hospital trial. *Applied Microbiology and Biotechnology.* Aug 2010;87(5):1875-1879.

12. Patnaik P. Handbook of Inorganic Chemicals: McGraw-Hill; 2003.

13. Santo CE, Lam EW, Elowsky CG, et al. Bacterial Killing by Dry Metallic Copper Surfaces. *Applied and Environmental Microbiology.* Feb 2011;77(3):794-802.

14. Singh A, Krishna V, Angerhofer A, Do B, MacDonald G, Moudgil B. Copper Coated Silica Nanoparticles for Odor Removal. *Langmuir.* 2010/10/19 2010;26(20):15837-15844.

15. Theodore JS, Mary Elizabeth J. The Effect of Copper on the Growth of Bacteria Isolated from Marine Environments. *Limnol Oceangr.* 1957;2(1):33-36.

16. Yan J, Buckley AM, Greenblatt M. The preparation and characterization of silica gels doped with copper complexes. *Journal of Non-Crystalline Solids.* 1995;180(2-3):180-190.